Effect of Compatibilizer on the Crystallization, Rheological, and Tensile Properties of LDPE/EVOH Blends

SANG YOUNG LEE, SUNG CHUL KIM

Department of Chemical Engineering, Korea Advanced Institute of Science & Technology, 373-1, Kusung-Dong, Yusung-Gu, Taejon, 305-701, South Korea

Received 6 February 1997; accepted 27 October 1997

ABSTRACT: The effect of the compatibilizer on the crystallization, rheological, and tensile properties of low-density polyethylene (LDPE)/ethylene vinyl alcohol (EVOH) (70/30) blends was investigated. Maleic anhydride-grafted linear low-density polyethylene (LLD-*g*-MAH) was used as the compatibilizer in various concentrations (from 1 to 12 phr). The interesting effect of compatibilization on the crystallization kinetics of the blends was noted, and the correlation between the morphology and the rheological and tensile properties was also discussed. Morphological analysis showed that the blends exhibited a regular and finer dispersion of the EVOH phase when LLD-*g*-MAH was added. Nonisothermal crystallization exotherms of the compatibilized LDPE/EVOH blends showed the retarded crystallization of the dispersed EVOH phase, which probably resulted from the constraint effect of the grafted EVOH (EVOH-*g*-LLD) as well as the size reduction of the EVOH domains. The blends exhibited increased melt viscosity and storage modulus and also enhanced tensile properties with the addition of LLD-*g*-MAH, which seemed to be attributable to both dispersed particle-size reduction and improved interfacial adhesion. © 1998 John Wiley & Sons, Inc. J Appl Polym Sci 68: 1245–1256, 1998

Key words: low-density polyethylene (LDPE); ethylene vinyl alcohol copolymer (EVOH); maleic anhydride-grafted linear low-density polyethylene (LLD-*g*-MAH); retarded crystallization; constraint effect; interfacial adhesion

INTRODUCTION

In recent years, plastic containers with high barrier properties have been produced with a multilayer structure using a coextrusion technology. One alternative to the multilayer extrusion could be based on the use of a polymer blend system having dispersed lamellae of impermeable polymers.[1–7] The ethylene vinyl alcohol (EVOH)/low-density polyethylene (LDPE) system is one example that may be cited.[6,7] EVOH has excellent gas barrier properties but is weak against moisture. On the other hand, LDPE has good durability against moisture. Therefore, LDPE/EVOH blends could be ideal for packaging applications. However, the blending of the two polymers usually leads to immiscibility, and the desired properties cannot be achieved without use of the compatibilizer. Blends based on polyolefins have often been compatibilized by reactive extrusion, where functionalized polyolefins are used to form copolymers at the interface to improve the compatibility between the components. Copolymers that are formed *in situ* during the compounding process may reduce the interfacial tension and, hence, increase the adhesion between the phases, allowing a finer dispersion and a more stable morphology to be created.[8–19]

Polymer blends containing one component with a higher crystallization temperature as a finely

Correspondence to: S. C. Kim.

Journal of Applied Polymer Science, Vol. 68, 1245–1256 (1998)
 CCC 0021-8995/98/081245-12

dispersed droplet suspension sometimes exhibit retarded crystallization.[15–19] Such retarded crystallization phenomena have been studied in the uncompatibilized blend systems,[15] where the dispersed droplet sizes were controlled by altering the mixing conditions. These observations are not completely explained, and where explained, the explanations are, in part, not satisfying or contradictory. In general, the practical blends always contain compatibilizers which are added to control the morphology.

In this study, the effects of the concentration of the compatibilizer, LLD-*g*-MAH, on the crystallization and melting behavior, especially the retarded crystallization of the dispersed EVOH phase, of LDPE/EVOH blends are discussed, and the morphological, rheological, and tensile properties of the blends were also investigated.

EXPERIMENTAL

Materials

LDPE [M.I. (g/10 min, 190°C, 2160 g) = 0.3] and EVOH [ethylene content (mol %) = 32] were obtained from LG Chemical Ltd. (Taejon, South Korea) and the Kuraray Co. (Kurashiki, Japan), respectively, in pellet form. Maleic anhydride-grafted LLDPE (LLD-*g*-MAH, wt % of MAH = 0.1) used as the compatibilizer was obtained from Mitsui Petrochemical Industries, Ltd. (Tokyo, Japan).

Blend Preparation

In all blends, the weight ratio of LDPE/EVOH was 70/30, and the concentration of the compatibilizer (LLD-*g*-MAH) was 1, 3, 5, 7, 9, and 12 phr (parts per hundred concentration of the resin). An uncompatibilized LDPE/EVOH blend with the same weight ratio as the compatibilized blend was also prepared for comparison. The blends were prepared using a counterrotating twin-screw extruder (C. W. Brabender compounder DSK 42/7) operating at a constant rotating speed of 40 rpm and the temperature profile of 200, 220, 240, and 240°C. All components were premixed by tumbling and simultaneously fed into the twin-screw extruder. Because of the hygroscopic behavior, EVOH was carefully dried in a vacuum oven for 24 h at 60°C before blending.

Morphological Analysis

Morphological changes in the LDPE/EVOH blends with the addition of LLD-*g*-MAH were observed with a scanning electron microscope (SEM), Phillips 535M. The specimens were prepared by cryogenically fracturing a sample and the fracture surface was covered with a thin layer of gold.

Thermal Measurements

Thermal analysis was carried out under a nitrogen atmosphere by a DuPont thermal analyzer 2000 Model differential scanning calorimeter to study the influence of the LLD-*g*-MAH added to the blends on the crystallinity, melting, and nonisothermal crystallization of the LDPE/EVOH blends. The temperature was increased from 30 to 230°C at a rate of 10°C/min and held in the molten state for 5 min to erase the thermal history. The nonisothermal crystallization thermograms were obtained by cooling the samples at programmed rates. The selected cooling rates were 2, 4, 8, 12, and 16°C/min. The melting thermograms were obtained from the second heating with a heating rate of 10°C/min.

Rheological Measurements

The rheological properties of the blends were measured with a rotational rheometer (Physica RheoLab MC120) using a cone-and-plate arrangement with a plate radius of 25 mm and a cone angle of 1°. In all cases, the sample gap was 50 μm and the strain was maintained at 15%. The tests were carried out by varying the frequency from 0.1 to 100 rad/s at 240°C. All tests were conducted under a nitrogen atmosphere to prevent oxidation.

Tensile Tests

The tensile properties of the compression-molded sample were measured with a tensile tester (Instron Model 4202) at room temperature, following the procedure described in ASTM D638. A crosshead speed of 10 mm/min was used in all measurements.

RESULTS AND DISCUSSION

Morphological Characterization

The effect of the concentration of LLD-*g*-MAH on the morphology of the LDPE/EVOH (70/30) blends is shown in Figure 1. The uncompatibilized blend [Fig. 1(a)] shows large and coarse domains.

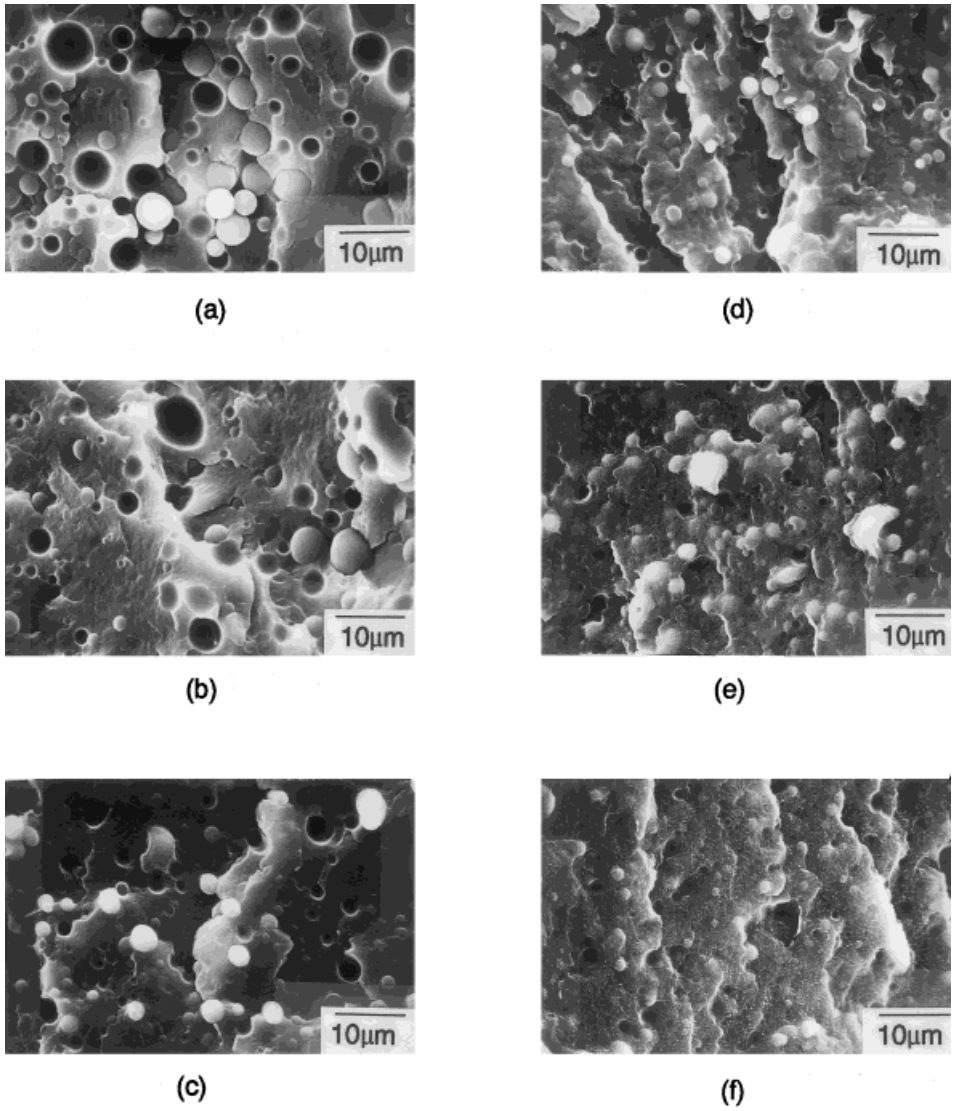

Figure 1 SEM photomicrographs of LDPE/EVOH (70/30) blends having various amounts of LLD-*g*-MAH: (a) without LLD-*g*-MAH; (b) 1 phr of LLD-*g*-MAH; (c) 3 phr of LLD-*g*-MAH; (d) 5 phr of LLD-*g*-MAH; (e) 9 phr of LLD-*g*-MAH; (f) 12 phr of LLD-*g*-MAH.

When LLD-*g*-MAH was added to the LDPE/EVOH (70/30) binary blend, the dimensions of the EVOH domains decreased about five to six times with increasing the amount of LLD-*g*-MAH up to 12 phr based on LDPE/EVOH. It is also evident that the presence of LLD-*g*-MAH improved the adhesion between the two phases, since the fractured EVOH domain changed from a spherical to an irregular shape as the amount of LLD-*g*-MAH was increased.

Crystallization and Melting Behavior

Figure 2 shows the cooling thermograms obtained at a cooling rate of 2°C/min of the LDPE/EVOH (70/30) blends having different amounts of LLD-*g*-MAH. The exothermic peak temperature of LDPE does not change significantly with the addition of LLD-*g*-MAH and stays at almost a constant temperature of about 98–99°C. However, in the EVOH phase, the addition of LLD-*g*-MAH causes a steady decrease of the exothermic peak temperature of the EVOH phase from 162°C for the uncompatibilized blend to 153°C for 12 phr of the LLD-*g*-MAH compatibilized blend. As the concentration of the LLD-*g*-MAH in the blend increases, more EVOH-grafted LLDPE (EVOH-*g*-LLD) may be formed *in situ* and the amount of EVOH-*g*-LLD in the EVOH-rich phase may in-

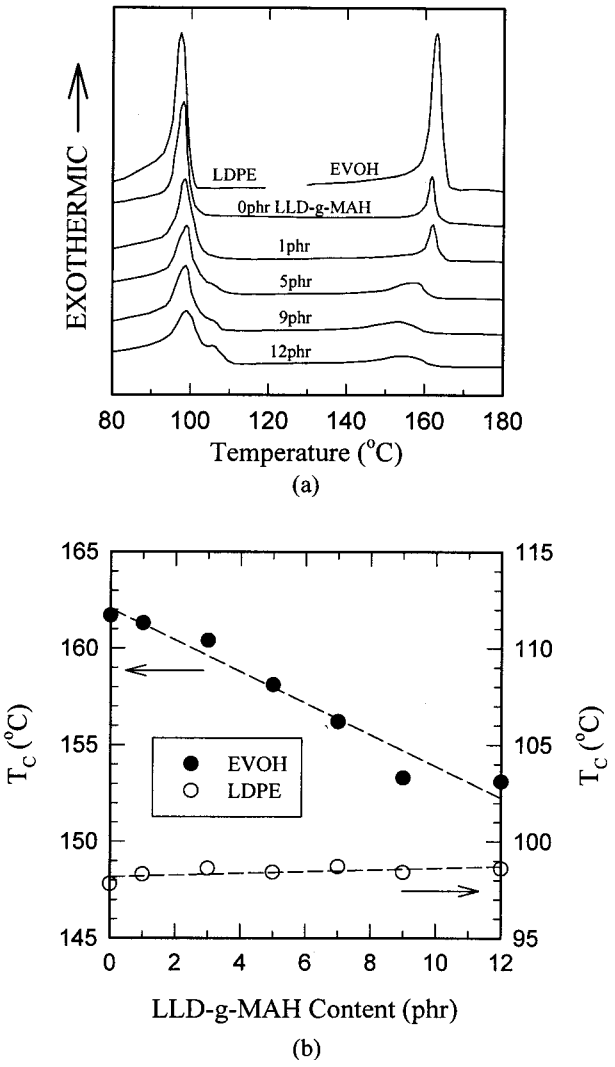

Figure 2 DSC cooling thermograms and crystallization peak temperatures (T_c) of LDPE/EVOH (70/30) blends having various amounts of LLD-*g*-MAH (cooling rate = 2°C/min): (a) DSC cooling thermograms; (b) crystallization peak temperature (T_c) versus LLD-*g*-MAH content.

crease. The EVOH-*g*-LLD present in the EVOH-rich phase may act as a polymeric diluent to retard the crystallization rate of EVOH and decrease the crystallization temperature of EVOH. Moon et al.[18] observed that in the compatibilized polypropylene (PP)/nylon 6 blends the crystallization temperature of the dispersed nylon 6 phase decreased as the concentration of the compatibilizer (PP-*g*-MAH) increased, whereas that of PP stayed at roughly a constant temperature.

To evaluate the relative miscibility of the compatibilizer, binary blends of LDPE/LLD-*g*-MAH and EVOH/LLD-*g*-MAH were made using the same twin-screw extruder mentioned in the Experimental section. Figure 3(a) shows that the crystallization temperatures of LDPE and LLD-*g*-MAH are not affected in the binary blend. However, Figure 3(b) shows that the crystallization

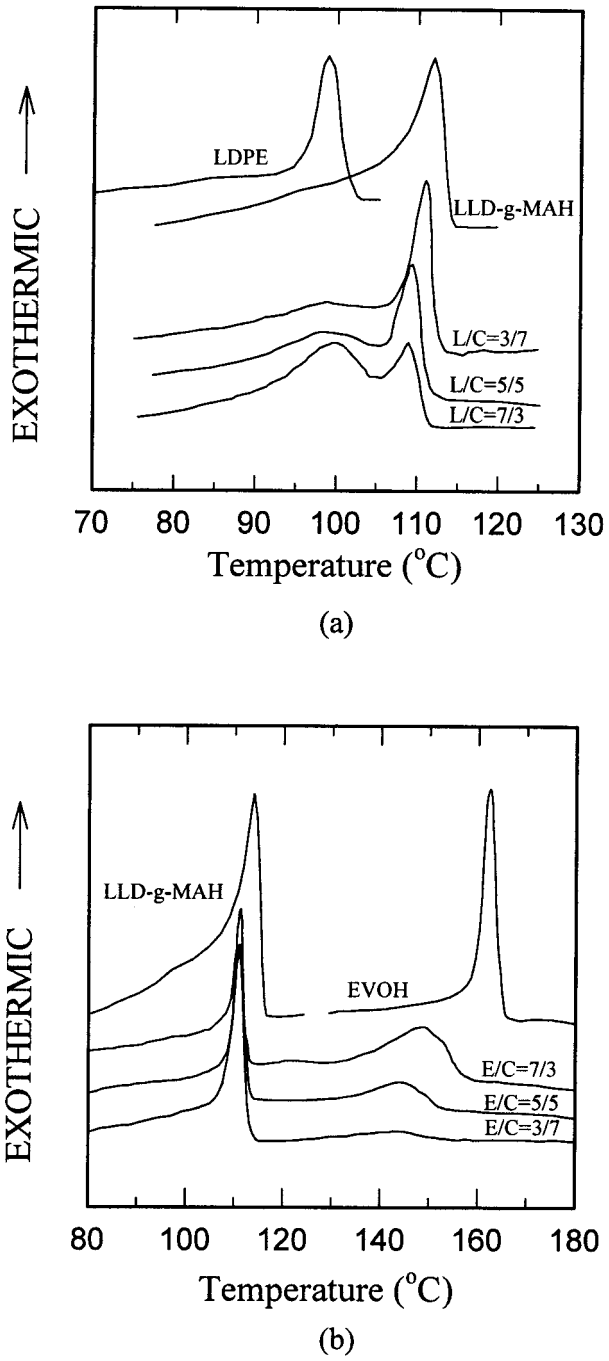

Figure 3 DSC cooling thermograms of binary blends (L: LDPE, E: EVOH, C: LLD-*g*-MAH, cooling rate = 2°C/min): (a) LDPE/LLD-*g*-MAH; (b) EVOH/LLD-*g*-MAH.

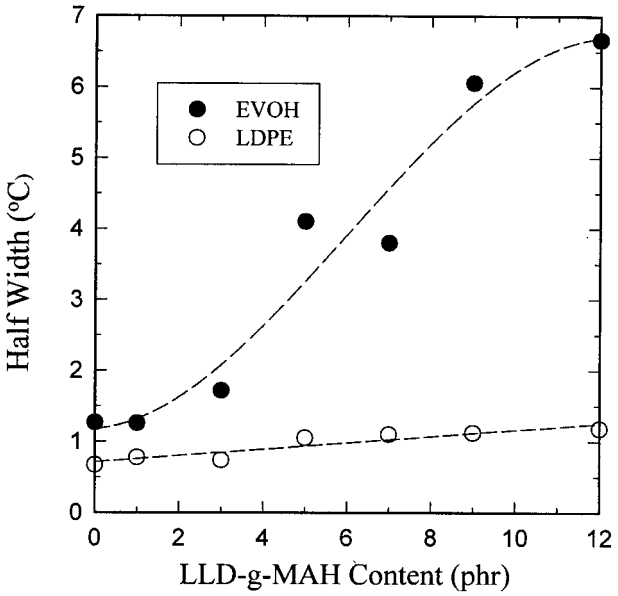

Figure 4 Half-width ($W_{1/2}$) of crystallization exotherms versus LLD-*g*-MAH content for both LDPE and EVOH in LDPE/EVOH (70/30) blends (cooling rate = 2°C/min).

peak temperature of EVOH in the EVOH/LLD-*g*-MAH blends decreases with increasing concentration of LLD-*g*-MAH. This indicates that there exist stronger interactions in the EVOH/LLD-*g*-MAH blends than in the LDPE/LLD-*g*-MAH blends and thus the retarded crystallization of EVOH is probably caused by the constraint effect of the grafted EVOH (EVOH-*g*-LLD). Willis et al.[14] reported similar results in PP/ionomer and nylon 6/ionomer binary blends. The retarded crystallization of nylon 6 and the positive deviation from the simple additivity rule in the viscosity/composition curve observed in the nylon 6/ionomer blends also indicated that stronger interactions existed between the ionomer and nylon 6.

The width of the crystallization exotherms measured at half-height, half-width ($W_{1/2}$), of the LDPE/EVOH (70/30) blends is given in Figure 4 as a function of the concentration of LLD-*g*-MAH. The half-width is a measure of the crystallite size distribution.[20] For LDPE, the $W_{1/2}$ value does not change much with the LLD-*g*-MAH concentration. For EVOH, a more pronounced increase in the $W_{1/2}$ with the LLD-*g*-MAH concentration was observed. This result would be expected if LLD-*g*-MAH is interfering with the crystallization of EVOH. Thus, a much wider distribution of EVOH crystallites occurs as a result of blending with LLD-*g*-MAH. Lee and Kim[7] studied the effect of the affinity difference of LLD-*g*-MAH for LDPE and EVOH on the morphology and oxygen barrier properties of LDPE/EVOH blends by changing the blending sequence. They observed the high affinity of LLD-*g*-MAH for EVOH, evidenced by the difference in morphology and oxygen permeability of the blends.

DSC heating thermograms and melting peak temperatures of the compatibilized LDPE/EVOH blends are shown in Figure 5. The melting temperature of LDPE is not changed much with the addition of LLD-*g*-MAH. However, for EVOH, increasing the amount of LLD-*g*-MAH decreases

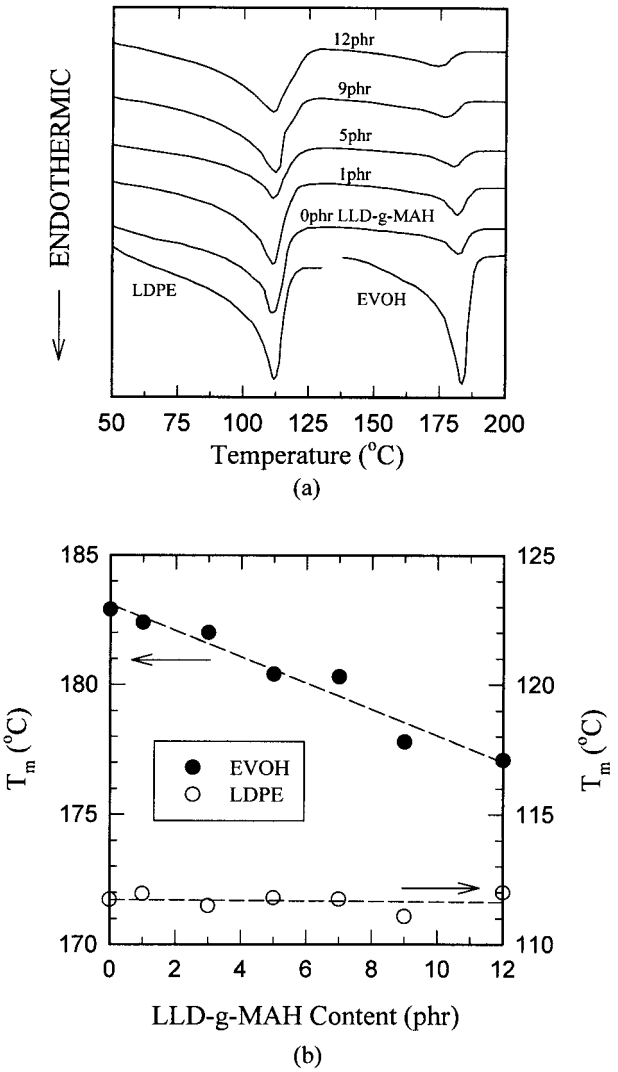

Figure 5 DSC second heating thermograms and melting peak temperatures (T_m) of LDPE/EVOH (70/30) blends having various amounts of LLD-*g*-MAH (heating rate = 10°C/min): (a) DSC second heating thermograms; (b) melting peak temperature (T_m) versus LLD-*g*-MAH content.

the melting temperature of EVOH. This is similar to the trend observed for the crystallization temperatures of the compatibilized LDPE/EVOH blends. The depressed melting temperature of EVOH in the compatibilized LDPE/EVOH blend may be due to the constraint effect of the grafted EVOH in the dispersed EVOH phase, indicating that the crystalline regions of EVOH are smaller and less perfect. These results are also evidenced by the heating thermograms of binary LDPE/LLD-*g*-MAH and EVOH/LLD-*g*-MAH blends (Fig. 6). Similar to the previous results, the melting temperature of LDPE in LDPE/LLD-*g*-MAH blends is not changed with increasing LLD-*g*-MAH, whereas that of EVOH in the EVOH/LLD-*g*-MAH blends decreases by the addition of LLD-*g*-MAH.

The plot of the heat of fusion for the compatibilized LDPE/EVOH blends is shown in Figure 7. The crystallinity of LDPE stays constant, while the crystallinity of EVOH in the blend decreases with the addition of the compatibilizer.

The crystallization and melting behavior of the compatibilized LDPE/EVOH blends are somewhat different from the PP/nylon 6 blends.[17,18] In the compatibilized PP/nylon 6 blends, the dispersed nylon 6 seemed to crystallize coincidentally with PP. It was probably due to the reduced particle size of nylon 6, since they found no melting temperature depression of nylon 6 and no change of crystallization and melting behavior of nylon 6 in the binary nylon 6/PP-*g*-MAH blends. However, in this study, besides the reduced domain size of EVOH, we observed the melting temperature depression of EVOH in the compatibilized LDPE/EVOH blends and also measured the changes of the crystallization and melting behavior of EVOH in the binary EVOH/LLD-*g*-MAH blends, which may indicate that the retarded crystallization of the dispersed EVOH phase in the compatibilized LDPE/EVOH blends resulted from the constraint effect of the grafted EVOH (EVOH-*g*-LLD) as well as the size reduction of the EVOH domains.

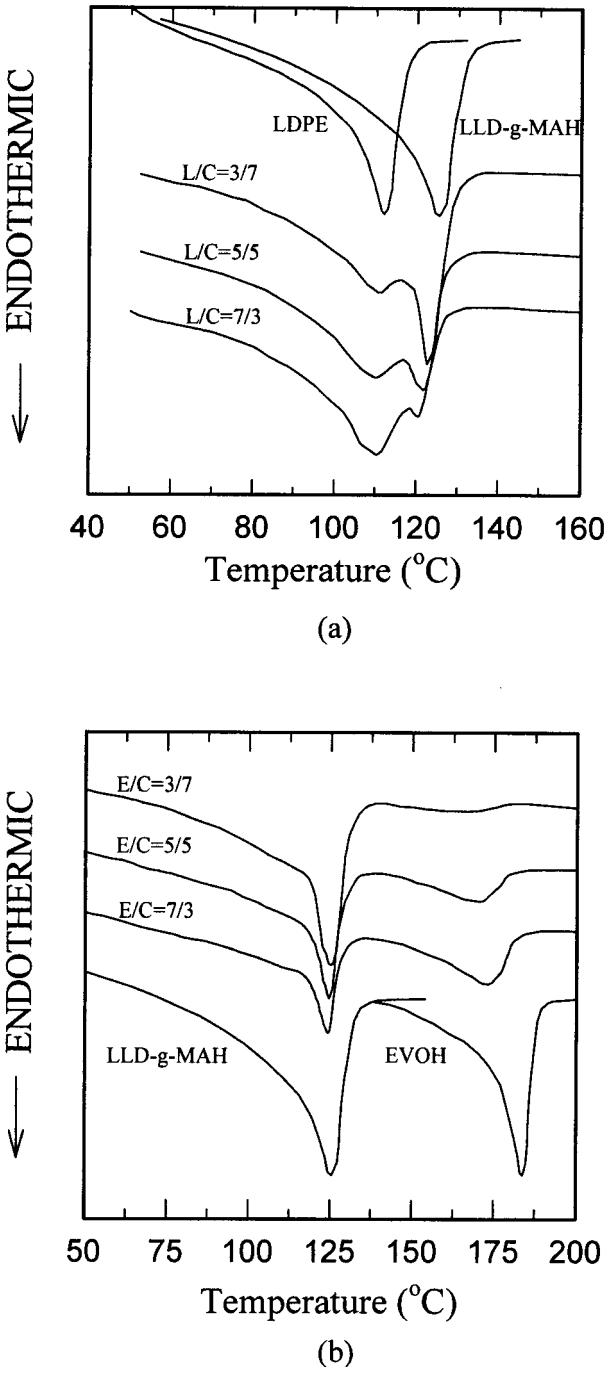

Figure 6 DSC second heating thermograms of binary blends (L: LDPE, E: EVOH, C: LLD-*g*-MAH, heating rate = 10°C/min): (a) LDPE/LLD-*g*-MAH; (b) EVOH/LLD-*g*-MAH.

Nonisothermal Crystallization Kinetics of the Compatibilized LDPE/EVOH Blends

The crystallization temperature upon cooling from the molten state is a characteristic value of a semicrystalline polymer. In programmed cooling, the crystallization temperature reflects the overall crystallization rate due to the combined effects of nucleation and crystal growth. There are several attempts reported in the literature to describe nonisothermal crystallization kinetics. Ziabicki[21,22] suggested that the maximum value of the rate constant corresponding to the crystallization peak temperature, K_{max}, can be calculated by the following equation:

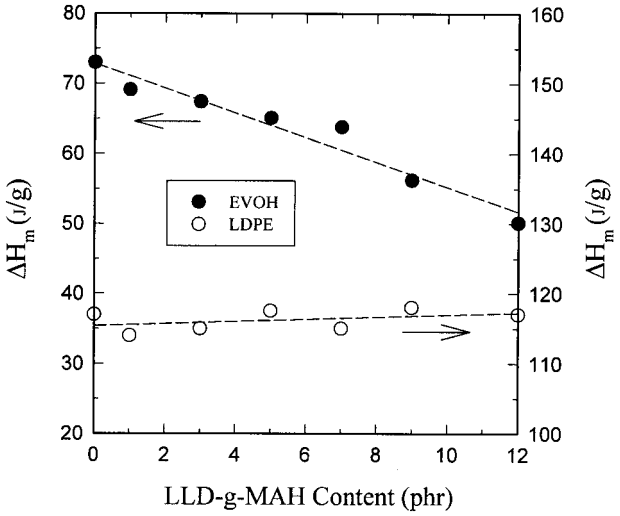

Figure 7 Heat of fusion (ΔH_m) versus LLD-*g*-MAH content for both LDPE and EVOH in LDPE/EVOH (70/30) blends (heating rate = 10°C/min).

$$K_{\max} = \frac{C_K}{t_{\max}} \quad (1)$$

where $t_{\max}$ is the time from the start of crystallization to reach the maximum rate of crystallization and C_K is the ratio of crystallinity before and after $t_{\max}$. A large value of $K_{\max}$ indicates that polymer crystallizes more rapidly. Nonisothermal crystallization exotherms observed in the DSC curve in the cooling runs (cooling rate = 2°C/min) were analyzed by Ziabicki's theory. The $K_{\max}$ values of LDPE and EVOH in the compatibilized LDPE/EVOH blends are plotted against the LLD-*g*-MAH content in Figure 8. It is seen that the crystallization rate of LDPE is not much affected by the presence of LLD-*g*-MAH. However, in contrast to what was observed for LDPE, the crystallization rate of EVOH decreases dramatically. This indicates that the crystallization process may be impeded by the constraint effect of EVOH-*g*-LLD in the EVOH phase as previously mentioned.

Considering these results, it is worth seeing the effect of LLD-*g*-MAH on the crystallization rate of the dispersed EVOH phase in the blends in more detail. The crystallization exotherms and relative crystallinity of EVOH in the uncompatibilized and compatibilized (9 phr of LLD-*g*-MAH) LDPE/EVOH blends at various cooling rates (2, 8, and 16°C/min) are presented in Figure 9. The relative crystallinity was calculated as a function of temperature using the relation

$$\frac{X(T)}{X_\infty} = \int_{T_0}^{T} \left(\frac{dH}{dT}\right) dT \Big/ \int_{T_0}^{T_\infty} \left(\frac{dH}{dT}\right) dT \quad (2)$$

where T_0 and T_∞, respectively, denote the onset and end temperatures of the crystallization of EVOH. Figure 9 shows that as the cooling rate increases the peak temperature decreases and the peak area also increases. The retarded crystallization of EVOH with 9 phr of the compatibilizer was obtained from the decreased crystallization temperature and broader crystallization exotherms of EVOH.

Khanna[23] and Zhang et al.[24] each introduced new parameters for characterizing the crystallization rate. Khanna proposed the crystallization rate coefficient (CRC), defined as $|\Delta\beta/\Delta T_C|$ (β is the cooling rate), which can be obtained from the slope of the cooling rate versus T_c. As indicated by Khanna, the higher the value of CRC, the higher the crystallization rate. The crystallization rate parameter (CRP) proposed by Zhang et al. is defined as $|\Delta(1/t_{1/2})/\Delta\beta|$ [$t_{1/2} = (T_{\text{in}} - T_{1/2})/\beta$; $t_{1/2}$ is the half-crystallization time, T_{in} is the onset temperature of crystallization, and $T_{1/2}$ is the half-crystallization temperature]. CRP can be obtained from the slope of the reciprocal of $t_{1/2}$ and the cooling rate plot. The faster the crystallization, the higher the slope. Figure 10 shows the reduction of the crystallization temperature with an increasing amount of the compatibilizer in the

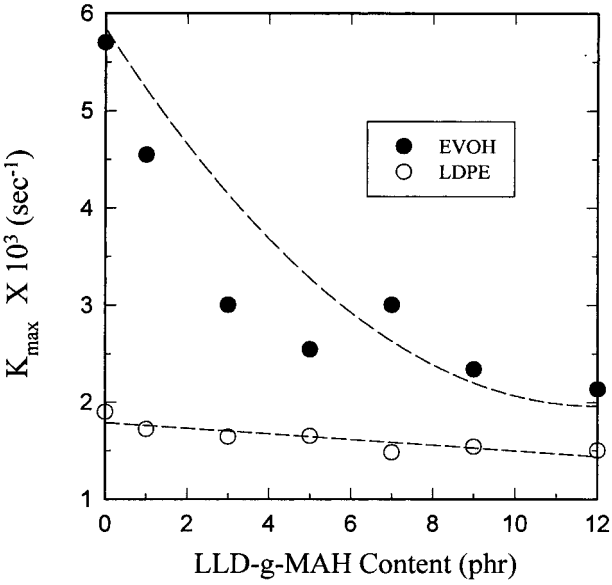

Figure 8 Maximum crystallization rate ($K_{\max}$) versus LLD-*g*-MAH content for both LDPE and EVOH in LDPE/EVOH (70/30) blends (cooling rate = 2°C/min).

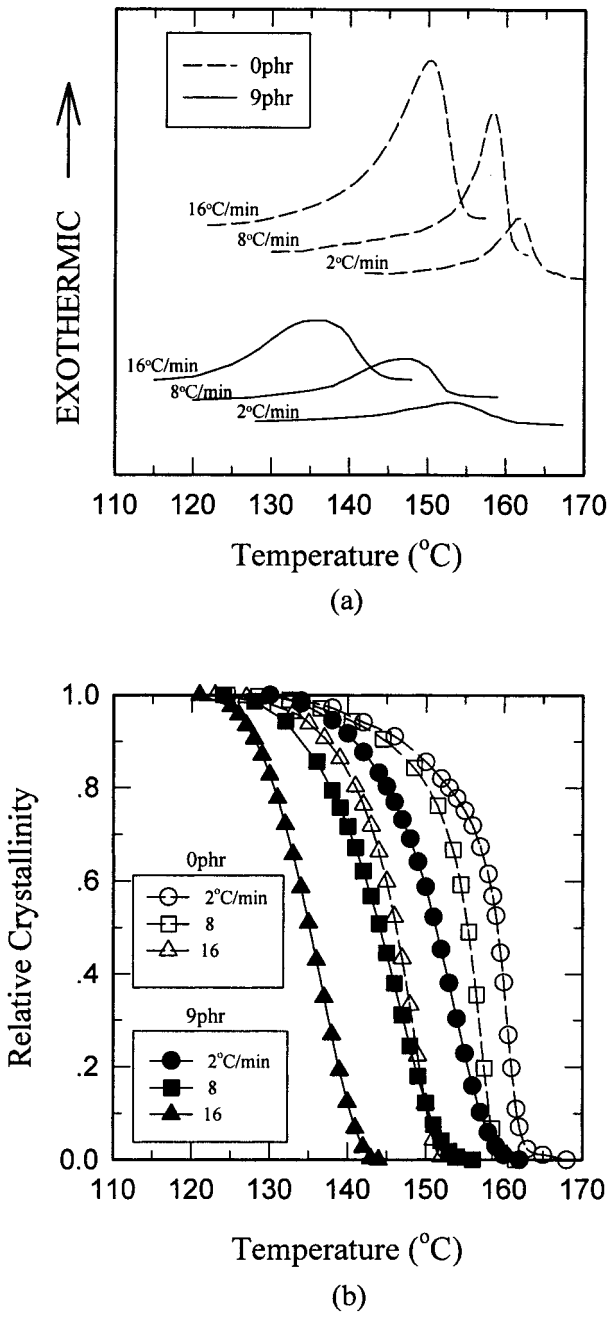

Figure 9 DSC cooling thermograms and relative crystallinity for EVOH in LDPE/EVOH (70/30) blends having no LLD-*g*-MAH and 9 phr of LLD-*g*-MAH at different cooling rates (cooling rates = 2, 8, 16°C/min): (a) DSC cooling thermograms; (b) relative crystallinity as a function of temperature.

compatibilized LDPE/EVOH blend. According to the treatment proposed by Khanna,[23] the cooling rate is plotted against the T_c of EVOH as shown in Figure 11(a), and the slope of the line, the CRC, can also be given as a function of the concentration of LLD-*g*-MAH [Fig. 11(b)]. From the results, we can find that the CRC value of EVOH decreases as the concentration of LLD-*g*-MAH increases, implying a lower crystallization rate of EVOH. Also, according to the method proposed by Zhang et al., CRP is obtained from the reciprocal of the $t_{1/2}$ of EVOH plotted against the cooling rate as shown in Figure 12(a). From Figure 12(b), we can find that the lower CRP value of EVOH at a higher concentration of LLD-*g*-MAH also indicates a lower crystallization rate of EVOH. In the compatibilized LDPE/EVOH blends, the variation of the CRC and CRP values of the dispersed EVOH phase represented quantitatively the retarded crystallization rate of EVOH.

Rheological Properties

The effect of the concentration of LLD-*g*-MAH on the complex viscosity of the LDPE/EVOH (70/30) blends is shown in Figure 13. In spite of the low viscosity of LLD-*g*-MAH, the blends show an increase in the viscosity with the addition of LLD-*g*-MAH. This is probably due to the grafting reaction of LLD-*g*-MAH and EVOH. In other words, when LLD-*g*-MAH is added to the blends, the interfacial adhesion between the dispersed EVOH and LDPE matrix phases increases as indicated by the SEM photomicrographs. The storage modulus (G') of the compatibilized LDPE/EVOH

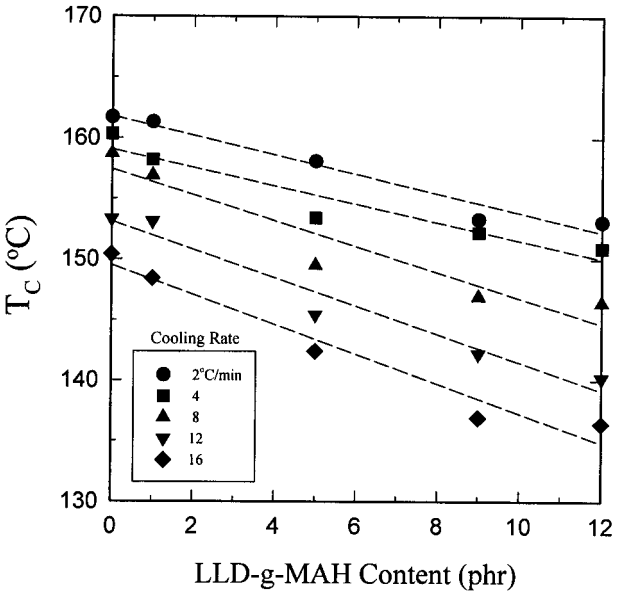

Figure 10 Crystallization peak temperature (T_c) of EVOH in LDPE/EVOH (70/30) blends versus compatibilizer (LLD-*g*-MAH) content at different cooling rates.

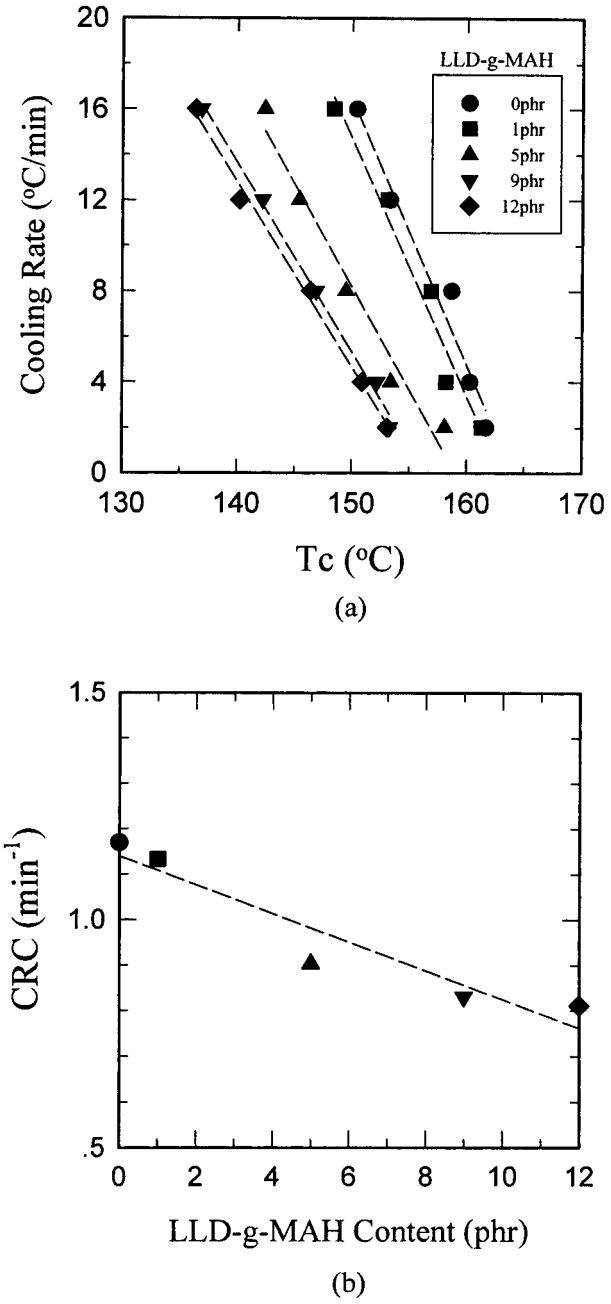

Figure 11 Effect of compatibilization on T_c and CRC for EVOH in LDPE/EVOH (70/30) blends: (a) cooling rate versus T_c; (b) CRC versus LLD-*g*-MAH content.

blends is plotted against the frequency in Figure 14. In this figure, the compatibilized blends show a higher storage modulus than that of the uncompatibilized blend over the entire frequencies. As shown in the above figures, the compatibilizer (LLD-*g*-MAH) can cause a great difference in rheological properties (complex viscosity and storage modulus) compared to the uncompatibilized blend. This is due to the increased interaction between the two phases by the presence of the compatibilizer.[8,9,25,26]

Tensile Properties

The effect of LLD-*g*-MAH on the tensile properties of the LDPE/EVOH (70/30) blends is shown in Figure 15. The addition of a compatibilizer has been shown to be a method of improv-

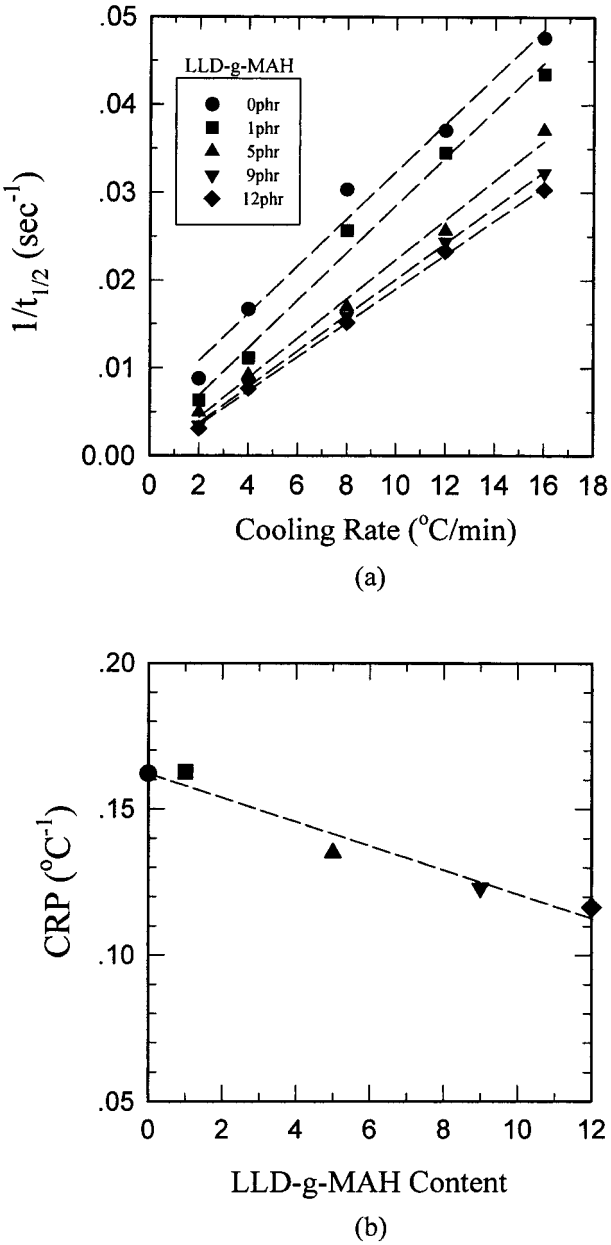

Figure 12 Effect of compatibilization on $t_{1/2}$ and CRP for EVOH in LDPE/EVOH (70/30) blends: (a) $t_{1/2}$ versus cooling rate; (b) CRP versus LLD-*g*-MAH content.

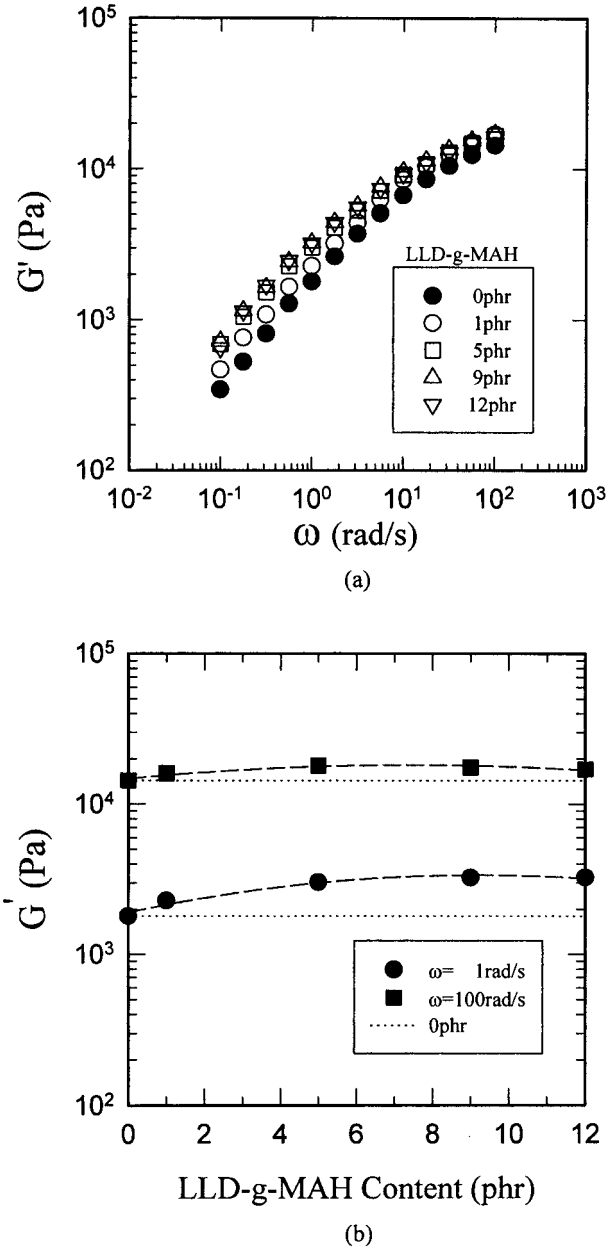

Figure 13 Effect of compatibilization on complex viscosity (η^*) of LDPE/EVOH (70/30) blends: (a) complex viscosity (η^*) versus frequency (ω); (b) complex viscosity (η^* at ω = 1 and 100 rad/s) versus LLD-*g*-MAH content.

ing the mechanical properties of the immiscible blends.[13–16,25,26] In Figure 15, it is seen that the tensile strength and elongation of the compatibilized blends are improved considerably relative to those of the uncompatibilized blend. The low value of elongation observed for the uncompatibilized blend can be attributed to the presence of a large EVOH domain with poor adhesion to the matrix. The increase of tensile properties in the compatibilized blends is probably related to the presence of LLD-*g*-MAH. This acts as an effective compatibilizer between the dispersed EVOH and LDPE matrix. It is likely that the addition of LLD-*g*-MAH yields a finer dispersity of the dispersed EVOH phase and stronger adhesion between the

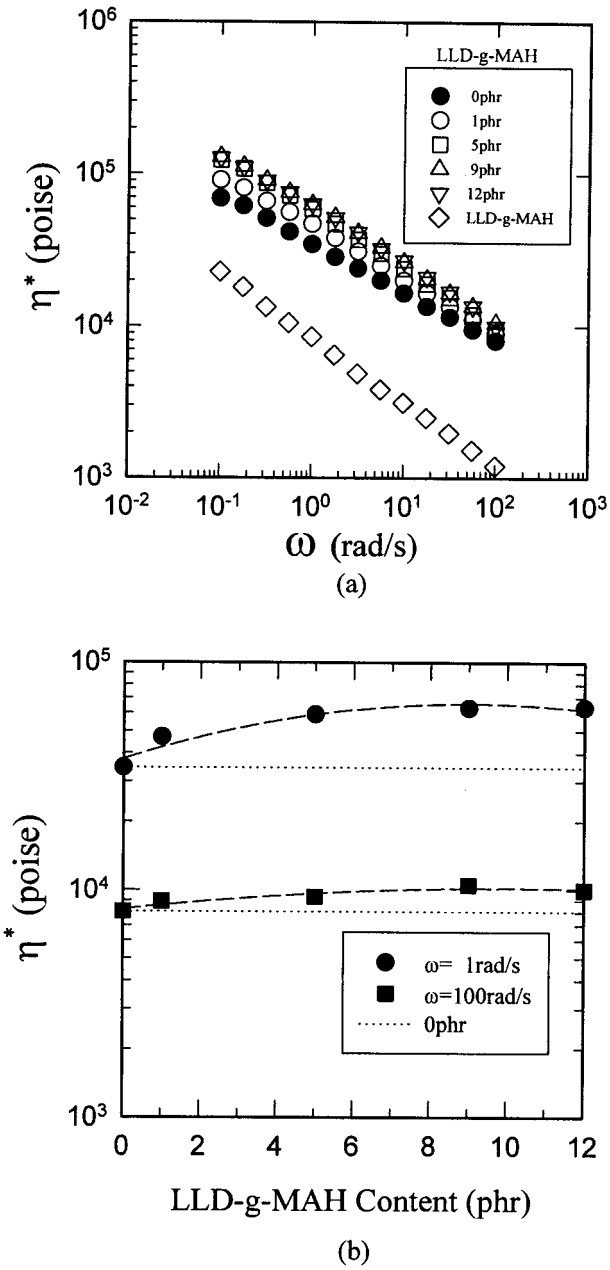

Figure 14 Effect of compatibilization on storage modulus (G') of LDPE/EVOH (70/30) blends: (a) storage modulus (G') versus frequency (ω); (b) storage modulus (G' at ω = 1 and 100 rad/s) versus LLD-*g*-MAH content.

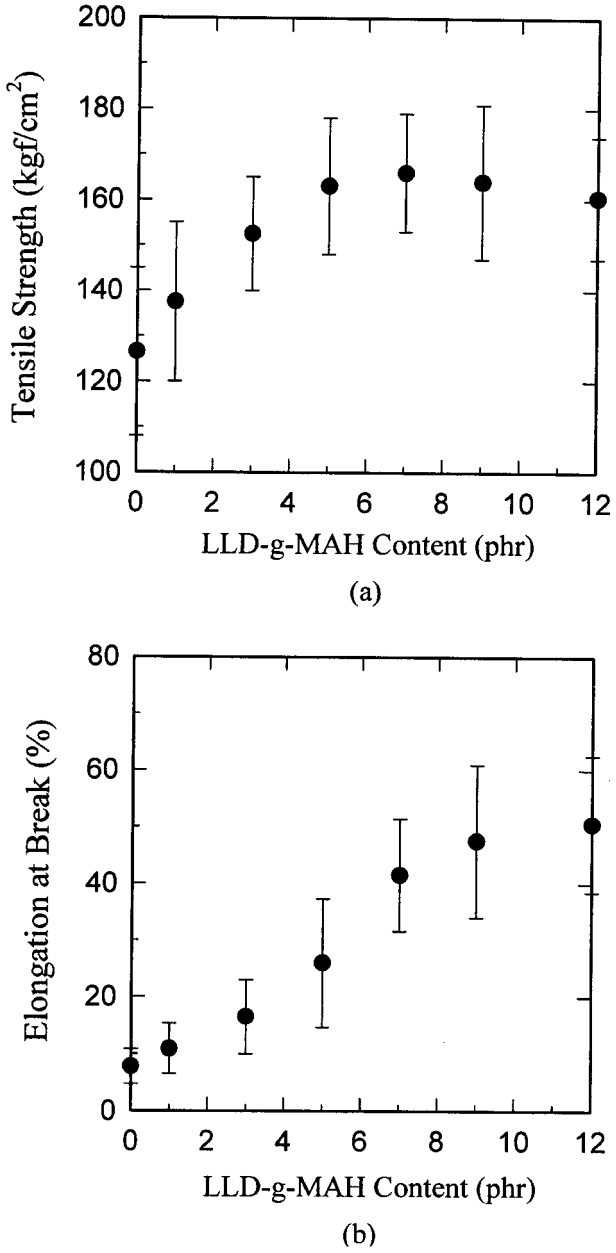

Figure 15 Effect of compatibilization on tensile properties of LDPE/EVOH (70/30) blends: (a) tensile strength; (b) elongation at break.

EVOH and LDPE phases, contributing to the improvement of the tensile properties of the compatibilized blends.

CONCLUSIONS

In this study, we investigated the effect of the compatibilization with LLD-*g*-MAH on the properties of immiscible LDPE/EVOH (70/30) blends. The results led to the following conclusions:

1. When the compatibilizer (LLD-*g*-MAH) was added to the LDPE/EVOH binary blend, the dimensions of the EVOH domains decreased by about five to six times with increasing the amount of LLD-*g*-MAH up to 12 phr.
2. The crystallization and melting behavior were significantly affected by the presence of LLD-*g*-MAH. The crystallization temperature of EVOH showed a trend of a steady decrease as the concentration of LLD-*g*-MAH increased, whereas that of LDPE stayed at a roughly constant temperature. The wider half-width ($W_{1/2}$) of the crystallization exotherms of EVOH than that of LDPE was measured. The melting temperature depression of EVOH in the compatibilized LDPE/EVOH blends and changes of the crystallization and melting behavior of EVOH in the binary EVOH/LLD-*g*-MAH blends may indicate that the retarded crystallization of the dispersed EVOH phase in the compatibilized LDPE/EVOH blends resulted from the constraint effect of the grafted EVOH (EVOH-*g*-LLD) as well as the size reduction of the EVOH domains.
3. The nonisothermal crystallization kinetics of the compatibilized LDPE/EVOH blends was studied. The lower K_{max}, CRC, and CRP values of EVOH at a higher concentration of LLD-*g*-MAH indicated the retarded crystallization rate of the dispersed EVOH phase.
4. The addition of LLD-*g*-MAH into LDPE/EVOH blends resulted in an increase in the melt viscosity and storage modulus of the blend, which was due to the increased interaction between the LDPE and EVOH phases by the presence of the compatibilizer.
5. Both a dispersed domain size reduction and an enhanced interfacial adhesion effect seemed to contribute to the improvement of the tensile properties in the compatibilized LDPE/EVOH blends.

REFERENCES

1. P. M. Subramanian, *Polym. Eng. Sci.,* **25,** 483 (1985).
2. P. M. Subramanian and V. Mehra, *Polym. Eng. Sci.,* **27,** 663 (1987).

3. G. W. Lohfink and M. R. Kamal, *Polym. Eng. Sci.,* **33,** 1404 (1993).
4. M. R. Kamal, M. Garmabi, S. Hozhahr, and L. Arghyris, *Polym. Eng. Sci.,* **35,** 41 (1995).
5. R. Gopalakrishnan, J. M. Schultz, and R. M. Gohil, *J. Appl. Polym. Sci.,* **56,** 1749 (1995).
6. S. Y. Lee and S. C. Kim, *Int. Polym. Process,* **11,** 238 (1996).
7. S. Y. Lee and S. C. Kim, *Polym. Eng. Sci.,* **37**(2), 463 (1997).
8. L. A. Utracki, Ed., *Polymer Alloys and Blends—Thermodynamics and Rheology,* Carl Hanser Verlag, Munich, 1990.
9. D. R. Paul and S. Newman, Eds., *Polymer Blends,* Academic Press, New York, 1978.
10. F. Ide and A. Hasegawa, *J. Appl. Polym. Sci.,* **18,** 963 (1974).
11. S. Wu, *Polym. Eng. Sci.,* **27,** 335 (1987).
12. B. K. Kim, S. Y. Park, and S. J. Park, *Eur. Polym. J.,* **27,** 349 (1991).
13. C. C. Chen and J. L. White, *Polym. Eng. Sci.,* **33,** 923 (1993).
14. J. M. Willis, B. D. Favis, and C. Lavallee, *J. Mater. Sci.,* **28,** 1749 (1991).
15. H. Frensch, P. Harnischfeger, and B. J. Jungnickel, in *Multiphase Polymer: Blends and Ionomers,* L. A. Utracki and R. A. Weiss, Eds., ACS Symposium Series 395, American Chemical Society, Washington, DC, 1989.
16. R. Holsti-Miettinen, J. Seppala, and O. T. Ikkala, *Polym. Eng. Sci.,* **32,** 868 (1992).
17. O. T. Ikkala, R. M. Holsti-Miettinen, and J. Seppala, *J. Appl. Polym. Sci.,* **49,** 1165 (1993).
18. H. S. Moon, B. K. Ryoo, and J. K. Park, *J. Polym. Sci. Polym. Phys.,* **32,** 1427 (1994).
19. H. K. Kim and S. C. Kim, *Polym. Adv. Technol.,* **1,** 325 (1990).
20. A. K. Gupta and V. B. Gupta, *J. Appl. Polym. Sci.,* **27,** 4669 (1982).
21. A. Ziabicki, *Appl. Polym. Symp.,* **6,** 1 (1967).
22. A. Jeziorny, *Polymer,* **19,** 1142 (1978).
23. Y. P. Khanna, *Polym. Eng. Sci.,* **30,** 1615 (1990).
24. R. Zhang, H. Zheng, X. Loy, and D. Ma, *J. Appl. Polym. Sci.,* **51,** 51 (1994).
25. H. C. Kim, K. H. Nam, and W. H. Jo, *Polymer,* **34,** 4043 (1993).
26. J. D. Lee and S. M. Yang, *Polym. Eng. Sci.,* **35,** 1821 (1995).